SUPPLEMENTAL FIGURES

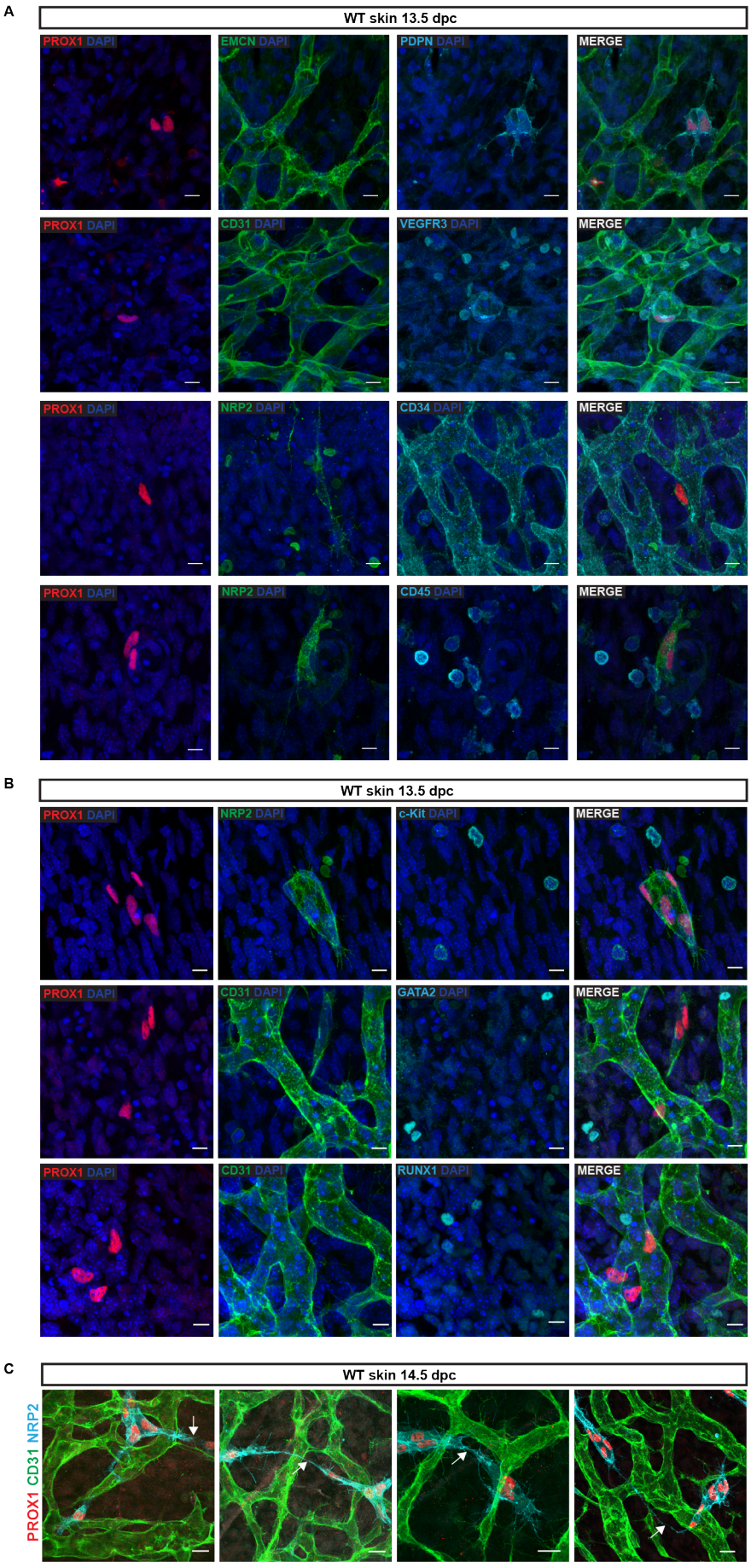

SUPPLEMENTAL FIGURE 1

Supplemental Figure 1: Characterisation of LEC clusters.

(A and B) Whole mount immunostaining of WT skins at 13.5 dpc for indicated proteins. Scale bars, 10 µm. (C) Whole mount immunostaining of WT skins at 14.5 dpc for CD31 (green), PROX1 (red) and NRP2 (blue). Arrows indicate filopodial contact extensions between LEC clusters and between LEC clusters and sprouting vessels. Scale bars, 20 µm. All images correspond to maximum intensity projections.

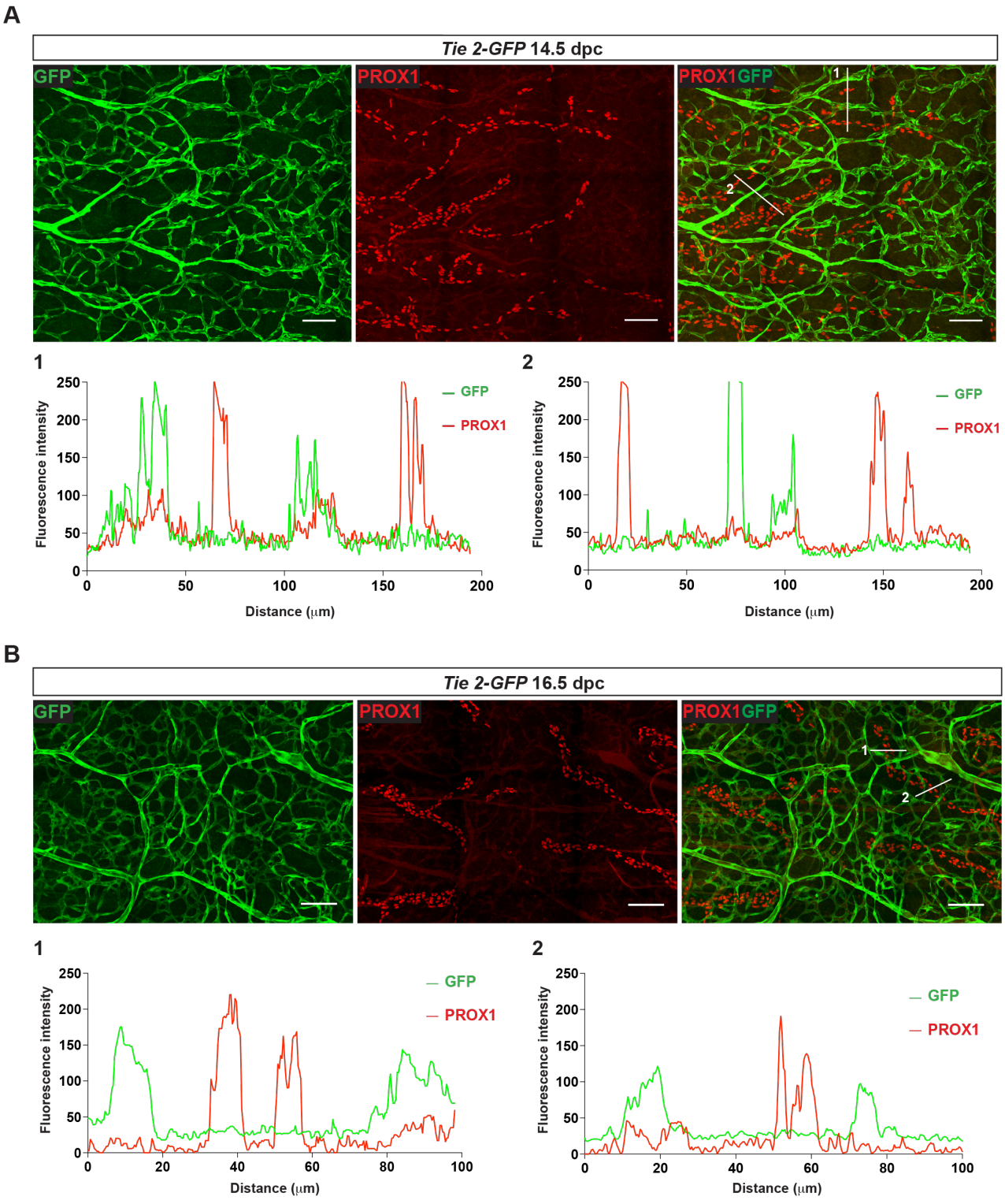

SUPPLEMENTAL FIGURE 2

Supplemental Figure 2: *Tie-2* is not express in dermal LECs.

Whole mount immunostaining of *Tie2-GFP* embryonic skin at 14.5 dpc (A) and 16.5 dpc (B) for PROX1 (red) and GFP (green). Graphs represent the fluorescent intensity of PROX1 and GFP over two independent 200 μm (A) and 100 μm (B) line-regions (1 and 2). GFP is strongly expressed in BECs and not detected in LECs. Scale bars, 100 μm.

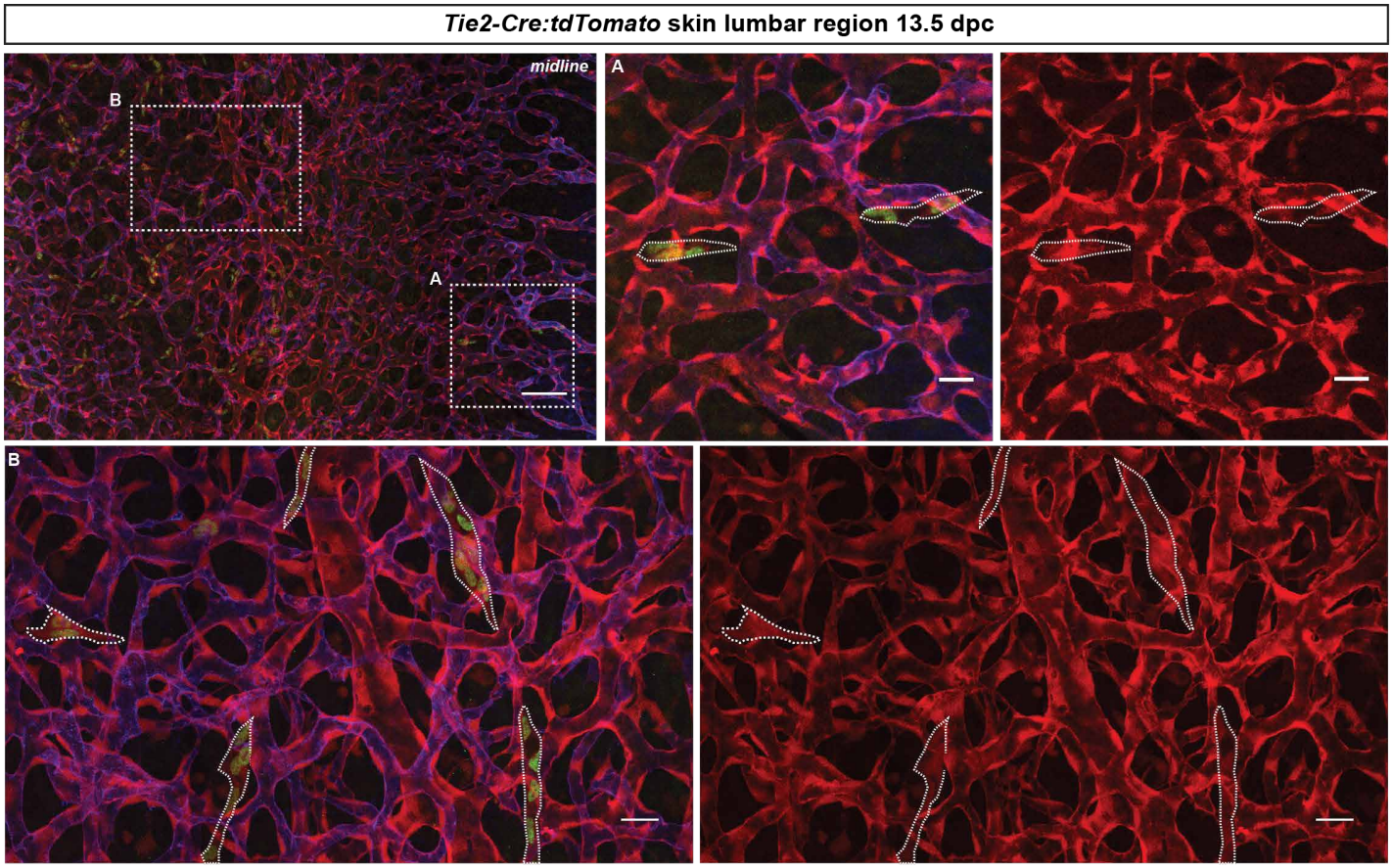

SUPPLEMENTAL FIGURE 3

Supplemental Figure 3: Lumbar LEC clusters have an endothelial origin.

Dermal whole mount immunostaining of *Tie2-Cre:tdTomato* skin (lumbar region) at 13.5 dpc for PROX1 (green) and EMCN (blue). In the lumbar region most LECs are tdTomato-positive. Scale bars 100 μm (top left image), 25 μm (all other images).

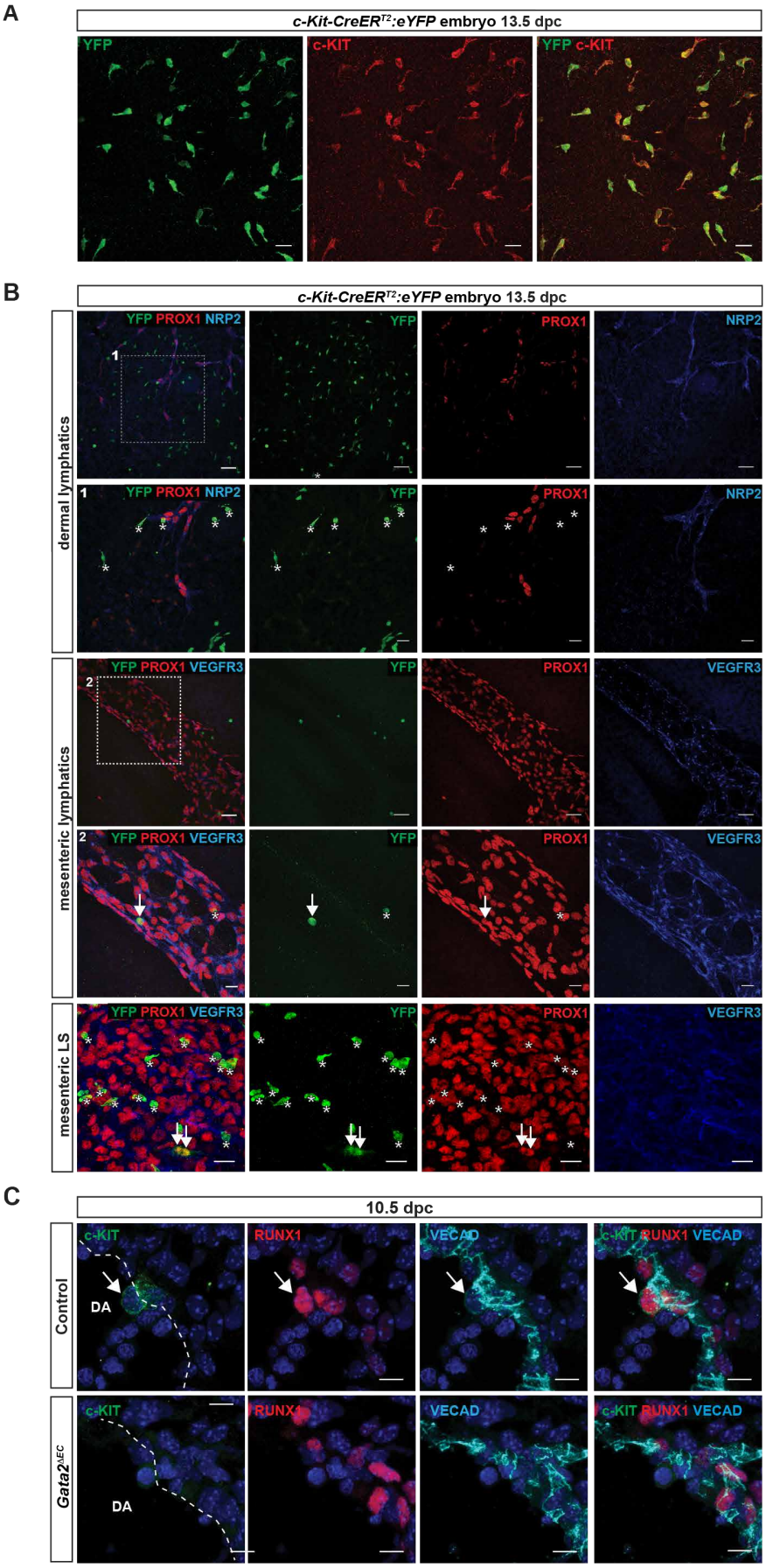

SUPPLEMENTAL FIGURE 4

Supplemental Figure 4: Hemogenic endothelium does not contribute to the formation of dermal lymphatics.

(A) Whole mount immunostaining of *c-Kit-CreERT2:eYFP* skin at 13.5 dpc for YFP (green) and c-KIT (red). YFP-positive cells are found in the skin and still express c-KIT protein. Scale bars, 20 μm (B) Whole mount immunostaining of *c-Kit-CreERT2:eYFP* skin (top) and mesentery (bottom) of the same embryo at 13.5 dpc for YFP (green), PROX1 (red) and NRP2 or VEGFR3 (blue). While scattered YFP-positive cells are found in the mesenteric lymphatic vessels and lymph sac (LS) (arrows), no YFP-positive cells where detected in the dermal lymphatics. Some YFP-positive/PROX1-negative cells are detected in the skin and mesentery (asterisks). In this experiments a single dose of tamoxifen was injected at 10.5 dpc. Boxed regions in upper panels (scale bars, 50 μm) are shown at higher magnification below (scale bars, 20 μm). (C) Transverse sections through the dorsal aorta (DA, dashed region) in the aorta-gonad-mesonephros region at 10.5 dpc stained for the hematopoietic stem cell markers RUNX1 (red) and c-KIT (green). Hematopoietic progenitor cells bud from the wall of the dorsal aorta (top, arrows) in littermate control embryos and are absent from the same region in *Gata2*$^{\Delta EC}$ embryos (bottom). Scale bars, 10 μm.

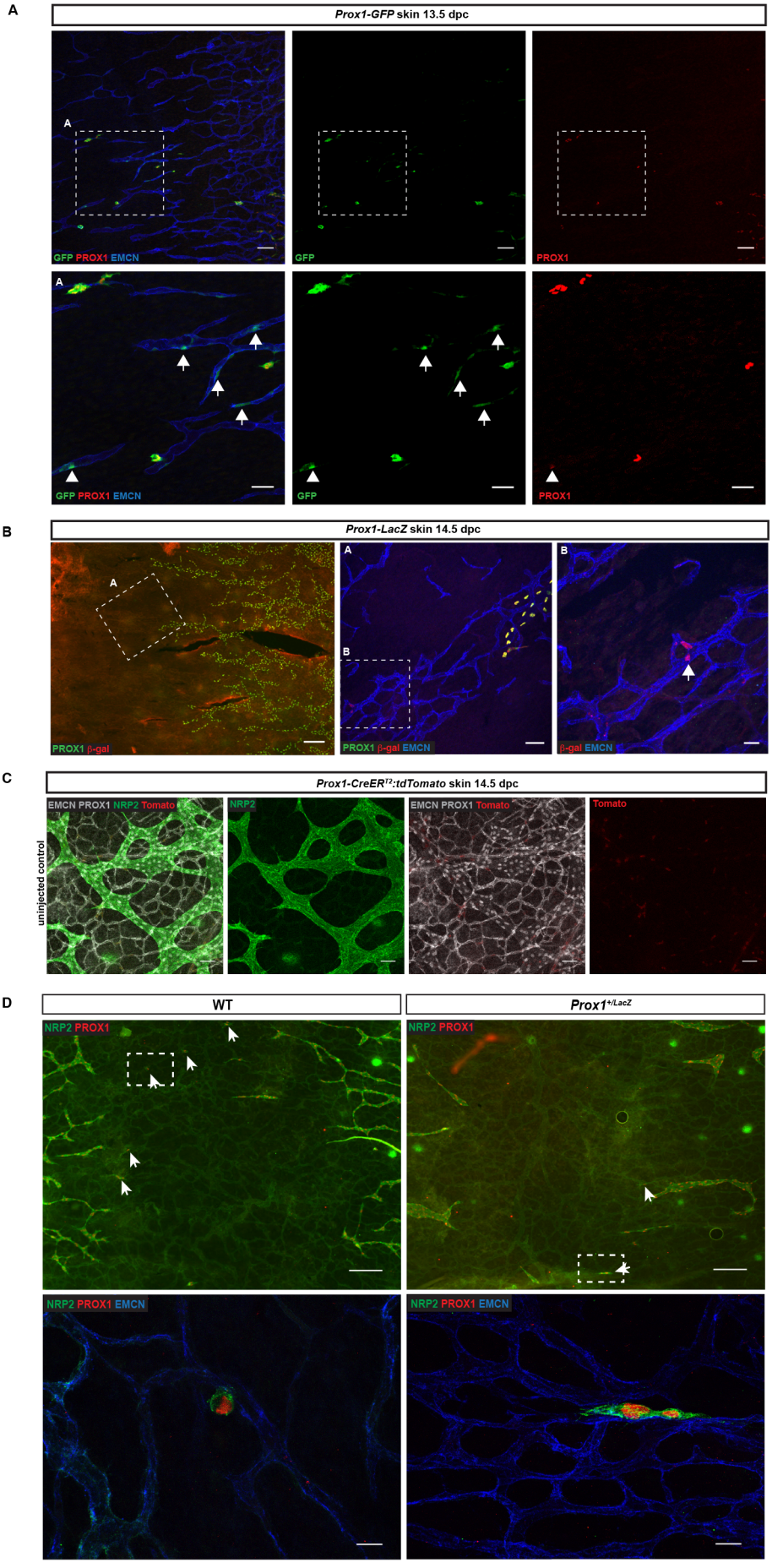

SUPPLEMENTAL FIGURE 5

Supplemental Figure 5: Characterisation of PROX1 expression in the dermal blood vascular capillary plexus. (A) Whole mount immunostaining of *Prox1-GFP* embryonic skin at 13.5 dpc for PROX1 (red), GFP (green) and EMCN (blue). GFP low cells are detected in the blood vascular plexus (arrows). Arrowhead depicts an endothelial cell that is GFP-positive and PROX1 protein low, suggesting the recent induction of PROX1 expression. Boxed regions in upper panels (scale bars, 50 μm) are shown at higher magnification below (scale bars, 20 μm). (B) Whole mount immunostaining of *Prox1-LacZ* embryonic skin at 14.5 dpc for PROX1 (green), β-gal (red) and EMCN (blue). Sparse β-gal-positive cells are detected in the blood vascular plexus (boxed region, arrow). Scale bars, 200 μm (left panel), 50 μm (middle panel), 20 μm (right panel). (C) Whole mount immunostaining of uninjected control *Prox1-CreERT2:tdTomato* skin for PROX1 (grey), EMCN (grey) and NRP2 (green) at 14.5 dpc. Scale bars, 50 μm. (D) Whole mount immunostaining of WT (left) and *Prox1+/LacZ* (right) embryonic skin at 14.5 dpc for PROX1 (red), NRP2 (green) and EMCN (blue). Arrows indicate LEC clusters. Boxed regions in upper panels are shown at higher magnification below. Scale bars, 200 μm (upper panels), 20 μm (lower panels).

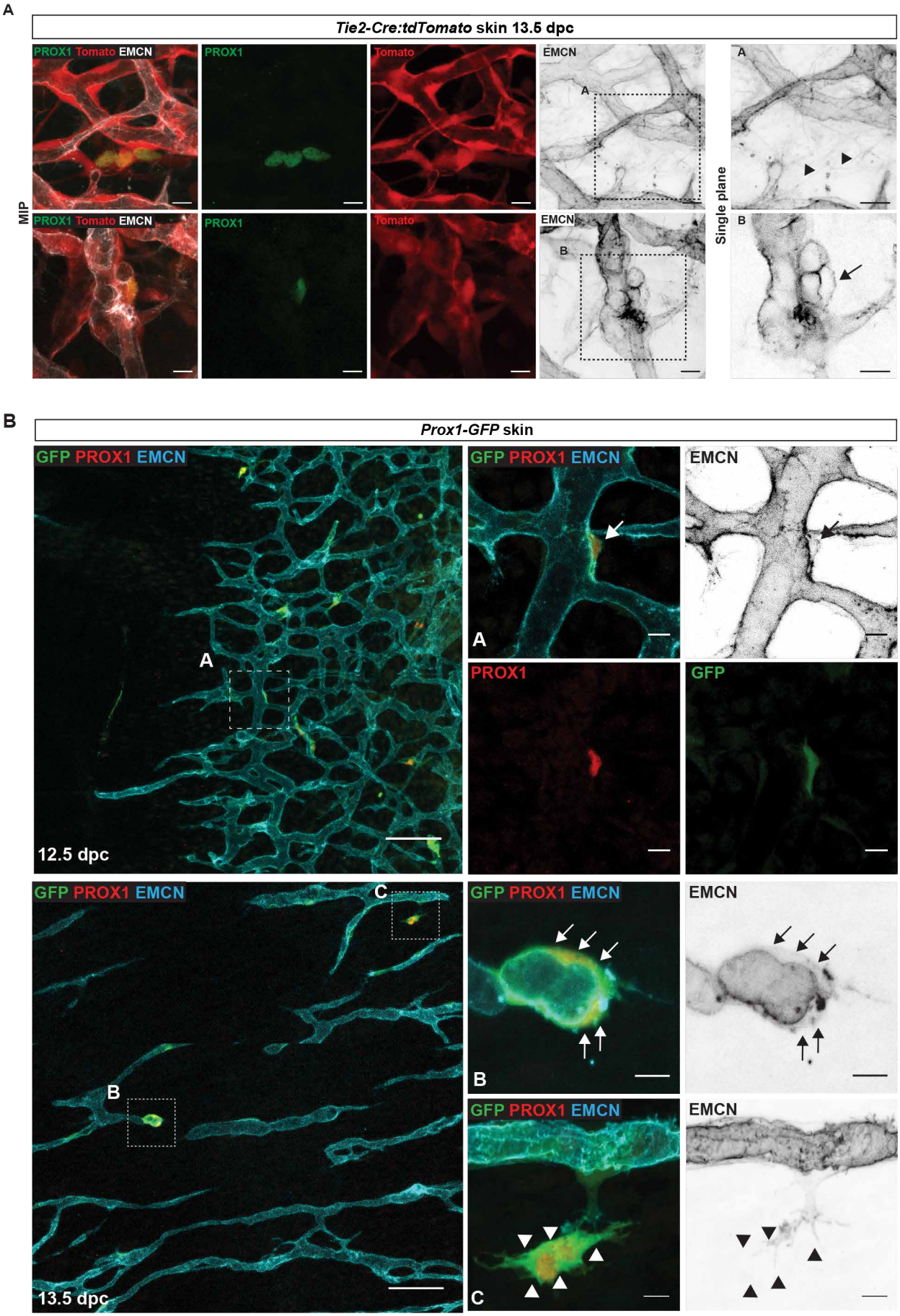

SUPPLEMENTAL FIGURE 6

Supplemental Figure 6: PROX1-positive/Endomucin-positive cells are found in the endothelial lining of the vessel wall. (A) Whole mount immunostaining of *Tie2Cre:tdTomato* skin at 13.5 dpc for PROX1 (green) and Endomucin (grey). While LEC clusters (arrowheads) are not expressing Endomucin (top panel), PROX1-positive cells (arrow) are found in the Endomucin positive plexus. Scale bars, 10 µm (B) Whole mount immunostaining of *Prox1-GFP* embryonic skins at 12.5 (top) and 13.5 dpc (bottom) for EMCN (blue), PROX1 (red) and GFP (green). Endogenous PROX1 is detected in the Endomucin-positive plexus (A and B), while LEC clusters are not expressing Endomucin (C). Boxed regions in left hand panels are shown at higher magnification in right panels. Arrows indicate PROX1-positive/Endomucin-positive cells and arrowheads indicate Endomucin-negative LEC clusters. Scale bars, 100 µm (left panels), 10µm (right panels).

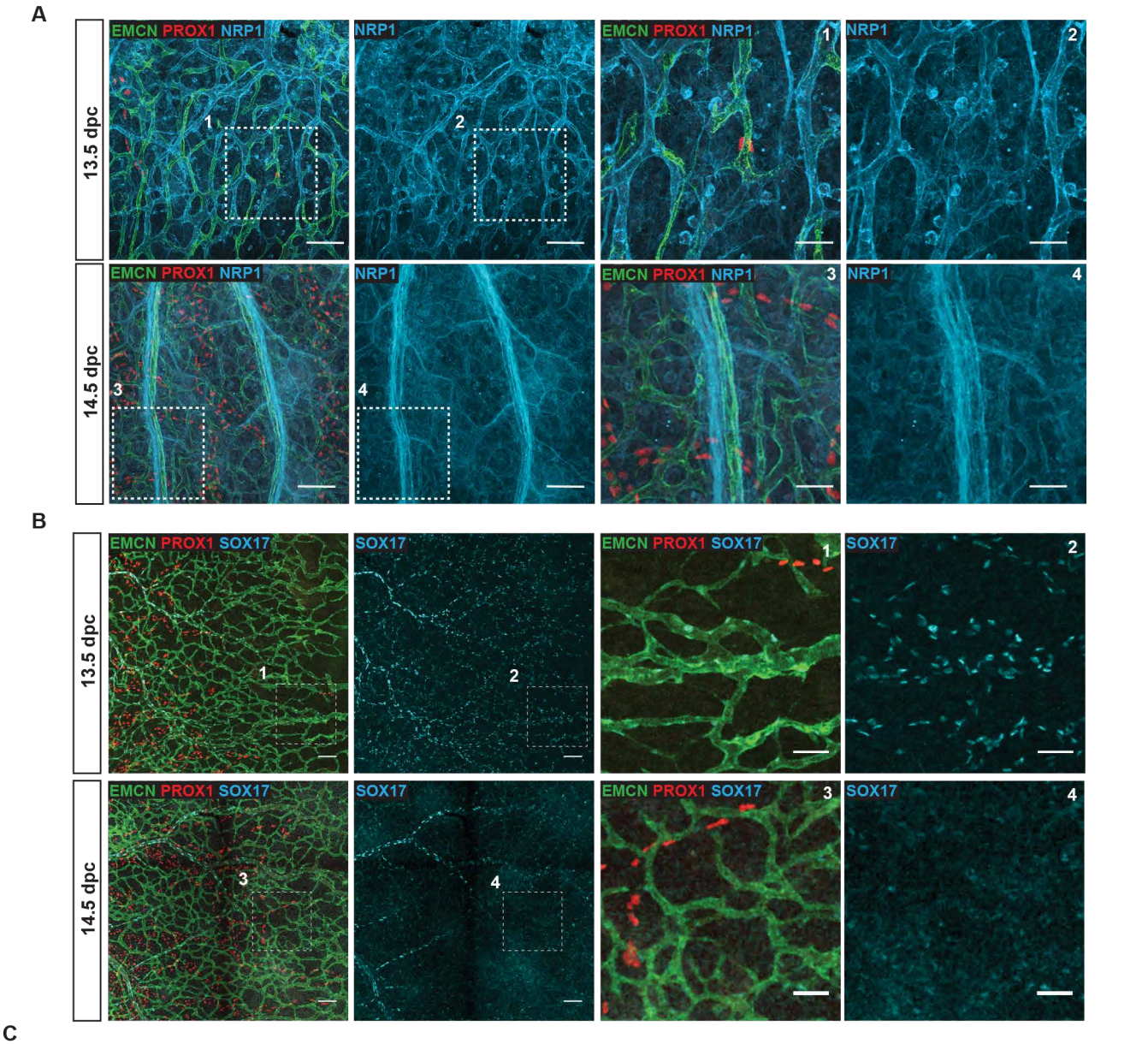

SUPPLEMENTAL FIGURE 7

Supplemental Figure 7: The dermal blood vascular capillary plexus exhibits markers of arterial and venous identity. (A) Whole mount immunostaining of embryonic skin at 13.5 dpc (top) and 14.5 dpc (bottom) for Endomucin (green), NRP1 (blue) and PROX1 (red). Scale bars, 100 μm (left panel), 50 μm (right panel). (B) Whole mount immunostaining of embryonic skin at 13.5 dpc (top) and 14.5 dpc (bottom) for PROX1 (red), Endomucin (green) and SOX17 (blue). Scale bars, 200 μm (left panel), 50 μm (right panel). While NRP1 and SOX17 are broadly expressed in the dermal blood plexus at 13.5 dpc, both arterial markers become restricted to arterioles at 14.5 dpc (A, B) Boxed regions in left panels are shown at higher magnification on right panels. (C) Whole mount immunostaining of embryonic skin at indicated time points for Endomucin (green) and Cx40 (red). Cx40 expression is weakly expressed in the blood vascular plexus at 13.5 dpc (arrows) and restricted to arterioles from 14.5 dpc. Endomucin expression is no longer expressed in arterioles from 15.5 dpc. Scale bars, 50 μm.

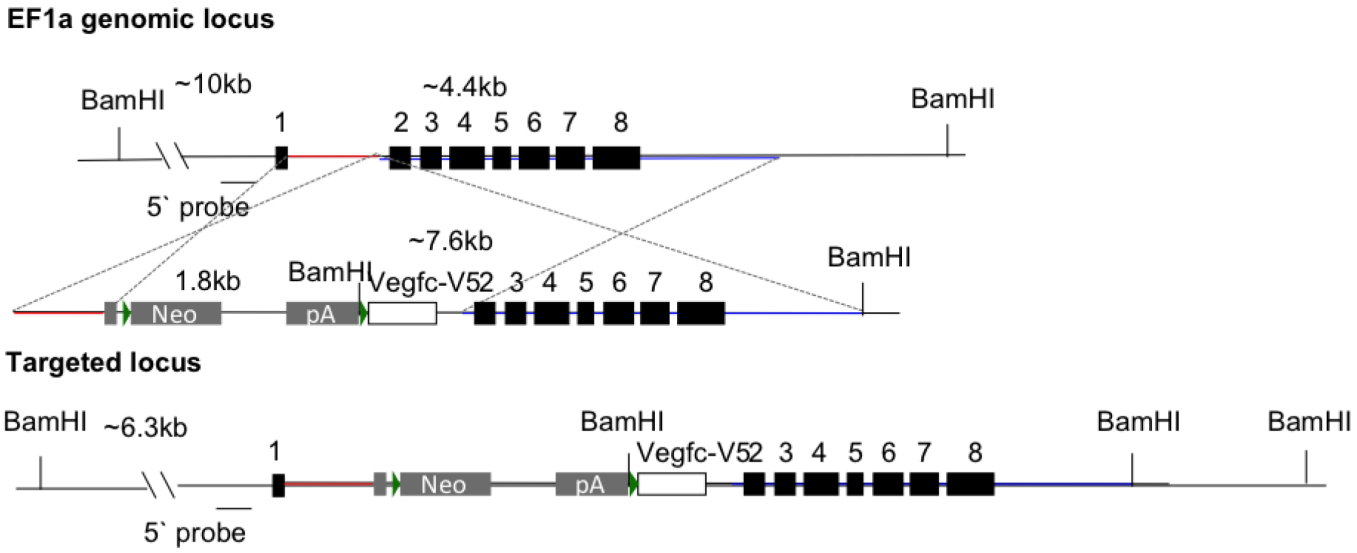

SUPPLEMENTAL FIGURE 8

Supplemental Figure 8: Generation of the *Vegf-cGOF* knock-in strain. The floxP flanked Poly(A) and neomycin cassette was inserted before the full length cDNA of mouse Vegfc with V5 tag. This construct was electroporated into W9.5 embryonic stem cells. The embryonic stem cells were then digested by BamHI, and genotyped by Southern blot analysis using the indicated probes. Correctly targeted embryonic stem cell clones were used to generate chimeric mice at St Jude Children's Research Hospital and Northwestern University.

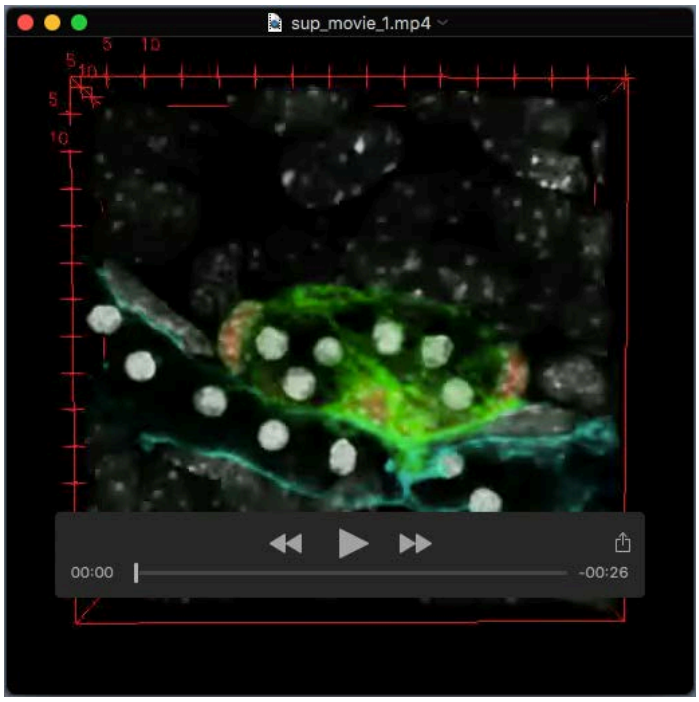

Supplemental Movie 1: Full z-stack images shown in Figure 5A. 3D volume rendering for Endomucin (blue), PROX1 (red), NRP2 (green) and DAPI allowing visualisation of the multicellular cluster that is budding from the Endomucin-positive blood vessel. Red blood cells are embedded inside the LEC cluster that still remains connected to the adjacent blood vessel.

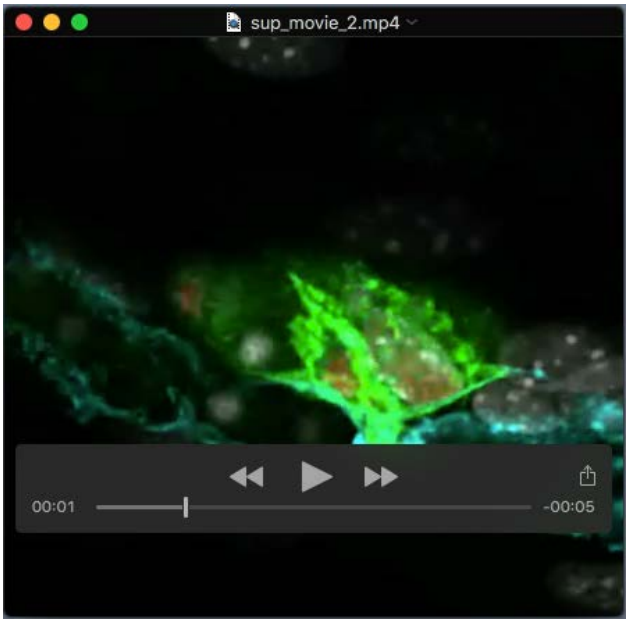

Supplemental Movie 2: Full z-stack images shown in Figure 5A.